

An Efficient Technique for making maps from Observations of the Cosmic Microwave Background Radiation

L. Piccirillo, G. Romeo, R. K. Schaefer and M. Limon
Bartol Research Institute, University of Delaware, Newark, DE, 19716

ABSTRACT

We describe a new technique for turning scans of the microwave sky into intensity maps. The technique is based on a Fourier series analysis and is inspired by the lock-in deconvolution used in experiments which typically sweep the sky continuously. We test the technique on computer generated microwave skies and compare it to the more standard map making technique based on linear algebra. We find that our technique is much faster than the usual technique and, in addition, does not suffer from the problem of memory limitations. Lastly we demonstrate that the technique works under real experimental conditions using observations of the moon.

Subject headings: Cosmic Background Radiation — Methods: data analysis

1. Introduction

One of the most important tests for models of the formation of cosmological structures is through the anisotropies in the cosmic microwave background radiation (CMBR). In order to identify which model of structure formation matches the pattern of temperature fluctuations one must compare the amplitude of fluctuations over a range of angular scales. Early CMBR experiments concentrated on comparing the temperatures of adjacent spots on the sky. As the sensitivities of experimental instruments improved, it was possible to entertain more sophisticated observing strategies. The results of the COBE satellite (see Bennett et al. 1996 and references therein) and the FIRS balloon experiment (Ganga et al. 1993) have demonstrated the superiority of making maps of the sky rather than simply finding temperature differences in a limited number of adjacent spots. In a map, one has a large number of temperature differences which can be found on a variety of different angular scales, which is a much better characterization of the intrinsic pattern in the sky than a measurement of the anisotropy on a single angular scale. The method of

map-making used by the COBE team consists of breaking up the sky into a large number (6144) of ~ 9 square degree pixels and making a large set of linear equations which must be inverted in order to have a map of the sky. As we would now like to explore the anisotropy on much smaller scales, this method of analysis would require us to break up the sky into a much larger number of pixels and solve a much larger number of linear equations to derive a map, with a considerable increase in computer time and memory. Recently, Wright et al., (1996), have suggested a new technique for producing mega-pixel maps from differential radiometer data. These authors claim that their technique has a computational cost that grows in the slowest possible way with increasing angular resolution and number of map pixels. CPU time and dimension of the RAM is proportional to the number of pixels. We will show that our approach has a CPU time also proportional to the number of pixels but the dimension of the RAM is kept constant. The inspiration for the method to be described here comes from the fact that the lock-in deconvolution technique - used in all sorts of differential CMBR measurements - can be used to directly determine the Fourier components of the temperature pattern on the sky (see also Netterfield et al. 1996). In this paper we develop this idea and test it on computer generated microwave sky (with and without added noise). The paper is organized as follows. In section 2, we describe our technique. In section 3, we describe how we generate our microwave skies for testing. In section 4, we compare our analysis technique with that used in making the COBE sky maps, and show a reconstructed map of the moon made from our observing site in Tenerife. We end the paper with some conclusions in section 5.

2. The Fourier approach

We assume that our CMB anisotropy experiment is performed by throwing the beam an angle $\theta(t)$ in the sky sinusoidally according to:

$$\theta(t) = \theta_0 \sin(\omega t) \tag{1}$$

where θ_0 is the maximum angular throw and $\omega/(2\pi)$ is the oscillation frequency. The output of our detector will be the signal $S(t)$. The fundamental idea for the inversion of data comes from the fact that given a periodic signal $S(t)$, it is possible to express it as a Fourier expansion, that is:

$$S(\theta(t)) = \frac{a_0}{2} + \sum_m a_m \cos(m\omega t + \phi) + \sum_m b_m \sin(m\omega t + \phi) \tag{2}$$

where ϕ is a phase, usually introduced by the detector electronics, which represents the phase delay between the sky signal and the voltage at the output of the detector. For sake of simplicity ϕ can be assumed to be zero. The coefficients of the expansion are given by

$$\begin{aligned} a_m &= \frac{2}{N} \sum_i s_i \cos(m\omega t_i) \\ b_m &= \frac{2}{N} \sum_i s_i \sin(m\omega t_i) \end{aligned} \quad (3)$$

where N is the number of points sampled per cycle of the sinusoid, s_i is the i -th signal collected in the i -th time interval t_i . Notice that the above coefficients are proportional to the output components of a lock-in amplifier using reference functions which are sines and cosines rather than a square wave. Since we are using a set of orthonormal functions to expand our signal, each harmonic component is independent. The phase ϕ can be chosen so that the signal $S(t)$ can be reconstructed by a series of sine (or cosine) terms. The orthogonal (quadrature) components, i.e. the cosine (or sine) terms will not contain any sky signal. It is evident from eq. 2 that the sky signal $S(\theta(t))$ is the sum of these components:

$$S(\theta(t_i)) = \frac{a_0}{2} + \sum_m a_m \cos(m\omega t_i + \phi) \quad (4)$$

$$R(\theta(t)) = \sum_m b_m \sin(m\omega t_i + \phi) \quad (5)$$

$R(\theta(t))$ contains all the spurious signals which are still coherent with the sinusoidal beam throw but are not produced by sky sources. Microphonics or glitches in the bolometers, for example, are easily controlled by studying $R(\theta(t))$.

Let us study the case of a typical ground-based experiment where the beam is thrown sinusoidally in the sky by wobbling either the primary or the secondary mirror of the telescope while the sky is drifting by. Let us suppose that N points are collected during every cycle. The sky intensity at the positions θ_i along the beam throw can be obtained by inserting in eq. 4 the times given by:

$$t_i = \frac{1}{\omega} \arcsin\left(\frac{\theta_i}{\theta_0}\right). \quad (6)$$

In summary, the basic idea consists of 1) sampling the signals from the detectors at high speed, 2) extracting the fundamental and higher harmonics coherent with the motion of the beam in the sky. Each of these harmonics provides rejection to all the noise sources (mainly from the detectors) which are not coherent, 3) making the inverse Fourier transform to recover the signal $S(\theta)$. Notice that the absolute intensity sky is recovered along the strip defined by the motion of the beam modulation. Differential experiments, with AC coupled detectors, will have $a_0 = 0$ and a differential map is obtained. It must be emphasized that this method is independent of the

observing pattern. Indeed, we have tried three different patterns, (see fig. 1), and all produced the same result.

3. Simulating the observations

Our aim is to show that we are capable of inverting the observational data in order to get a map of the sky emission. We will demonstrate this by using a synthesized microwave map of the sky. To generate the microwave skies for our simulations, we make use of the spherical harmonic expansion of the temperature field $T(\theta, \phi)$ on the sky

$$T(\theta, \phi) = T_0 \sum_{l,m} a_{lm} B_l Y_m^l(\theta, \phi) \quad (7)$$

where T_0 is the average background temperature, a_{lm} are the temperature anisotropy coefficients, B_l is the expansion of the experimental beam profile of the telescope, and $Y_m^l(\theta, \phi)$ are the spherical harmonics, (where θ is the declination and ϕ is the right ascension). The beam profile here is assumed to be Gaussian with a FWHM of 1 degree, so B_l is given by:

$$B_l = \exp \left[-1/2(l(l+1)(0.4247 \text{ FWHM})^2) \right] \quad (8)$$

From the above relation we see that the temperature sum (eq. 7) will be cut off for $l > 300$, so that we only include $l < 300$ in our sum. It is computationally easier for us to generate smoothed maps for simulating the differential measurements. We calculate all $Y_m^l(\theta, \phi)$ in steps of 0.33 degrees in both right ascension and declination over the range $17 \leq \delta \leq 35^\circ$, and $0 \leq RA \leq 360$ degrees, which would be appropriate for a mid-latitude scan of the zenith. We will simulate our observation on a part of this map. The a_{lm} are given random phases and Gaussian random amplitude using the variance $\langle |a_{lm}|^2 \rangle$ corresponding to the cold dark matter model, with a scale free spectrum $n=1$, a Hubble constant of $H_0 = 50 \text{ km s}^{-1} \text{ Mpc}^{-1}$, and a baryon fraction of 5%. The particular values of $\langle |a_{lm}|^2 \rangle$ were taken from Schaefer and de Laix (1996).

Once the map was obtained, we performed both a COBE like simulation, and a simulation with our new technique. In the COBE like simulation, we have two radiometers which perform a raster scan of the sky. While in the sky, and the radiometers are drifting, we calculated the positions of the two horns every 0.02 seconds, and then we read the temperature from the map. Finally, we took the difference between the two radiometers, and we inverted these data with the same procedure used in making the COBE maps (Lineweaver 1996, Janssen et al. 1992). According to the COBE method, we divided our patch of synthesized sky in pixels of equal area. Using + to denote the horn which read as positive the temperatures, and - for the other horn, then during the n-th observation we had

$$D_n = [T_{n+}(i) - T_{n-}(j)] \quad (9)$$

after performing N observations, then we can represent our data in matrix form, namely

$$\begin{pmatrix} D_1 \\ \dots \\ D_N \end{pmatrix} = \begin{pmatrix} 0 & 1 & 0 & \dots & 0 & -1 & 0 & \dots \\ \dots & \dots & \dots & \dots & \dots & \dots & \dots & \dots \\ 0 & 0 & -1 & 0 & 0 & \dots & 1 & \dots \end{pmatrix} \begin{pmatrix} T(1) \\ \dots \\ T(k) \end{pmatrix} \quad (10)$$

where N is the number of observations, and k is the number of pixels. The above can be rewritten more compactly as a matrix equation

$$\mathbf{D} = \mathbf{M}\mathbf{T} \quad (11)$$

Notice that the dimensions of \mathbf{M} are given by the number of observations and the number of pixels. The previous equation can be inverted, and we find the vector \mathbf{T} , that is

$$\mathbf{T} = \mathbf{A}^{-1}\mathbf{M}^T\mathbf{D} \quad (12)$$

where

$$\mathbf{A} = \mathbf{M}^T\mathbf{M} \quad (13)$$

As expected, the technique was extremely accurate since the correlation between the original map and the reconstructed map was 99.99%. On the same map, we also simulated three different strategies in order to test our Fourier based technique. In the first one, the telescope beam moves sinusoidally along the direction of the sky drift. In the second one, we allow the beam to move in a direction normal to the direction of the sky drift. Finally, we allowed the beam to describe circles in the sky. This last strategy has some interest for future satellite and/or balloon-borne experiments. In each of the above cases we were able to reconstruct the simulated map. To simulate the observations, the position (right ascension and declination) of the center of the beam was calculated for every point, while also allowing the sky to drift. Once the position was obtained, we read the temperature on the map with the same right ascension and declination. In the first simulation we used a frequency for the sinusoidal motion of 2.0 Hz, with 64 points sampled every cycle. This choice of parameters correspond to our Tenerife 1996 bolometer campaign (Piccirillo et al. 1996).

4. Inverting the data

Let us now illustrate our method for the inversion of maps for each of the three strategies of observation as shown in fig. 1. In the horizontal scan (fig. 1b) the beam center moves sinusoidally along the direction of the sky drift. By using eq. 4, where we considered only the first 6 harmonics, we are able to reconstruct the temperature at the beginning of every cycle, so that we get the temperature profile along a fixed declination; then by moving the beam center to a new declination, we obtain a two dimensional map of the sky. This strategy has some important limitations. First of all, the bi-dimensional map is obtained by joining strips at constant declination measured at different times. Atmospheric and/or detector drifts can be so large that they will destroy the correlation between different declinations. These problems can be greatly reduced by using either the normal scan or the circular scan. The reason is that these two techniques, and especially the circular one, are intrinsically bi-dimensional. A 2 dimensional map can be obtained in a time scale which could be chosen to be negligible with respect to both the atmospheric and the detector drifts. Let us first analyze the normal scan. Suppose that our telescope beam is centered at a declination of 23 degrees, that the peak to peak amplitude of the sinusoidal oscillation is 6 degrees and that 64 points are sampled every cycle. By using eq. 4, we will map the temperature profile along different parallels from $\delta = 20^\circ$ to $\delta = 26^\circ$. For instance, suppose that we want to map the temperature profile at 26 degrees, then the time which enters in eq. 4 is given by $t = \frac{16}{64}T$ which corresponds to the time at which the antenna is pointing at $\delta = 26^\circ$. Similarly, the profile for other declinations can be found by adjusting t accordingly. The same considerations will apply to the circular scan.

We can now discuss the results of our map making technique. In figure 2a we have the map used in our simulations, while in fig. 2b & 2c we have the reconstructed maps respectively with the COBE approach and our new technique. It is evident that COBE method is as accurate as our new approach. From the figures it can be seen that both techniques are extremely accurate, both generated maps which have a correlation with the original map very close to 100%. However, we must take into account the fact that the COBE approach has some disadvantages: first of all, it is slow when compared with our technique: to invert the same map it took about 4 hours of CPU time with the COBE like inversion, while it took 20 minutes with our method. Also, the method can be applied in real time so that it is possible to get a quick look at the maps when the data are still in the collection phase. The second and probably most important limitation of COBE inversion is the difficulty of obtaining high spatial resolution maps. As said previously, COBE method involves the use of matrices whose dimensions are given by the number of pixels and the number of observations. An increase in the map resolution means an increase in the matrix dimensions. The next generation of anisotropy satellite experiments expected to achieve sub-degree spatial resolution would face enormous computational problems in inverting huge matrices. It is possible to consider sub-matrices so that the matrix dimensions are reduced but the calculation involved would slow down the computation time. Our technique, on the other hand, does not involve any matrices, hence is fast and the resolution that can be realized is only limited

by the beam size.

We studied our technique in the presence of detector noise and on the higher resolution map. We introduced the instrumental noise at every point sampled and, for simplicity, we assumed it had a Gaussian distribution. To study a more realistic scenario, we simulated a mid-latitude balloon-borne experiment with bolometers having a noise of $200 \mu K/\sqrt{Hz}$. The instrumental beam size was 20' FWHM and the beam throw was a sinusoid of 80' peak to peak amplitude. We simulated a 10 hours flight on a map at 3' spatial resolution. This choice of parameters is very similar to the MSAM-2 experiment (Kowitt et al. 1995). The original and reconstructed map are visible in fig. 3a and 3b. Notice that the reconstructed map has also a 3' pixel size.

Lastly, we present an elementary application of the technique to real data. During our recent microwave observing campaign in Tenerife, (Piccirillo et al. 1996) we made observations of the moon for purposes of calibration. Due to the location of the moon in the sky over Tenerife, it was much easier to get an accurate measurement using a horizontal scan rather than a vertical one. We therefore can reconstruct a one-dimensional map of the moon using the techniques described in this paper. (To make a two-dimensional map, we would require additional scans at adjacent declinations.) In figure 4, we present our reconstruction of the moon map. As in the simulations, the moon is smoothed by our beamsize of 1.3° FWHM. Here we show the data from one channel with $\lambda = 2.1$ mm. We use 5 harmonics in the sum in eq. 4 to reconstruct the moon. For comparison we have made a simple simulation of what signal is expected from a moon (approximated as a uniform disk) smoothed by our Gaussian beam. We also express the simulation as a Fourier series with only 5 harmonics, which accounts for the apparent features at the moon's edges. We see that the mapping technique works quite well in this situation under real observing conditions.

5. Conclusion

From our simulations and our simple application to real data, we have demonstrated that this new technique, based on Fourier series works quite well. We learned that the most efficient observational strategy is the one where the beam center moves fast and explores the maximum amount of sky in the minimum time, compatible with the speed and noise of the detectors. From the comparison with the COBE approach, it seems that our method offers more advantages especially in terms of computer memory limitation and speed when we want to obtain sky maps at high spatial resolution. The relatively high speed of the algorithm will also allow the realization of efficient quick-look programs, i.e. real-time visualizations of the inverted data when the experiment is still in the phase of the data collection.

REFERENCES

- Bennett, C.L., *et al.*, 1996, *ApJ*, 464, 1
- Ganga, K.M., Cheng, E., Meyer, S., & Page, L., 1993, *ApJ* 410, L57
- Janssen, M. & Gulkis, S., 1992, *The Infrared and Submillimeter Sky After COBE*, Les Houches, France, p. 391
- Kowitt, M. S., *et al.*, 1995, *Astrop. Lett. & Comm.*, 32, 273
- Lineweaver, C., 1996, *Proc. of the 1994 BCSPIN Summer School*, World Scientific, Singapore (in press)
- Netterfield, B., *et al.*, 1996, Preprint astro-ph/9601197
- Piccirillo, L., *et al.*, 1996, in preparation.
- Schaefer, R. K., & de Laix, A. A., 1996, *ApJS*, 105, 1
- Wright, E.L., Hinshaw, G., Bennett, C.L., 1996, *ApJ*, 458, L53

6. FIGURE CAPTIONS

Fig. 1.— The three observing strategies discussed are shown. From the top to the bottom, they are: (a) vertical scan, (b) horizontal scan and (c) circular scan, all centered on declination δ .

Fig. 2.— The upper panel (a) is the original map. This is the computer generated map over which we performed both our simulations of the observations. It has already been smoothed with a Gaussian beam profile with $\text{FWHM} = 1$ degree. The pixels are $1/3$ of degree by $1/3$ of degree and contours are labelled in μK . Panel (b) is the reconstructed map by using COBE method. Panel (c) is the reconstructed map by using our Fourier based approach, and taking into account only the first 6 harmonics. The correlations between the reconstructed maps and the original one are both very close to 100 %.

Fig. 3.— The upper panel (a) is the higher resolution original map. The pixels are 0.05 degree by 0.05 degree. This map was used only to perform a Fourier simulation since the number of pixels is too large to perform a COBE-like simulation on our computer. The lower panel (b) is the Fourier reconstructed map using 9 harmonics. This last map has been obtained by adding an instrumental noise of $200 \mu K/Hz^{1/2}$. We simulated 10 hours of observations corresponding to a mid-latitude balloon-flight. The correlation between this map and the original map is about 93 %.

Fig. 4.— The reconstructed intensity map of the moon made using a horizontal scan through the center of the moon’s disk with our microwave telescope in Tenerife using the 2.1 mm wavelength channel. The light line is a simulation of the expected signal of the moon seen through a Gaussian beam of 1.3° FWHM. Both the map and the simulated moon use only 5 harmonics in the Fourier series, leading to rounded moon “edges”.

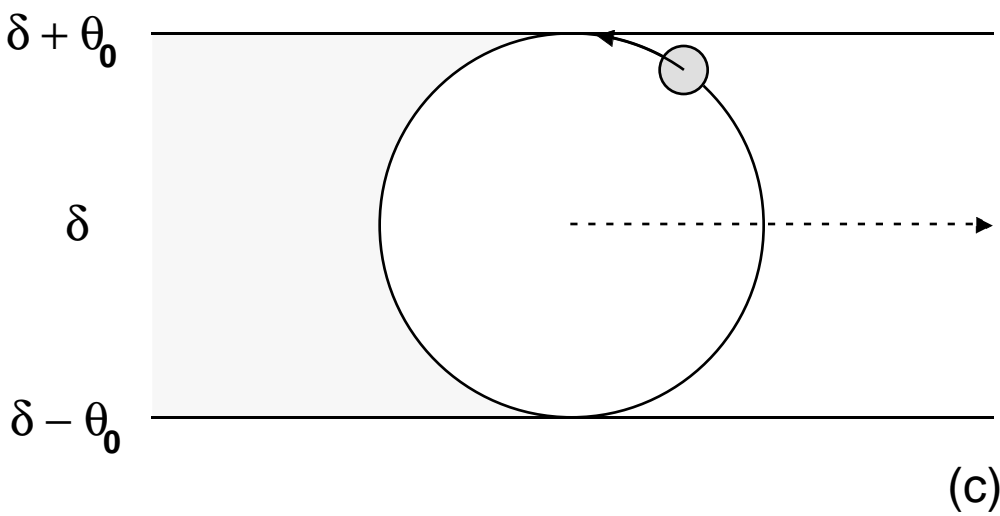
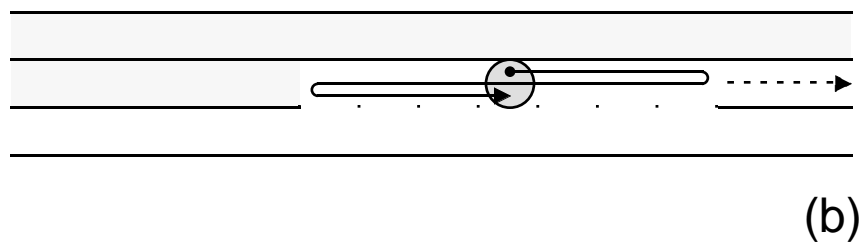
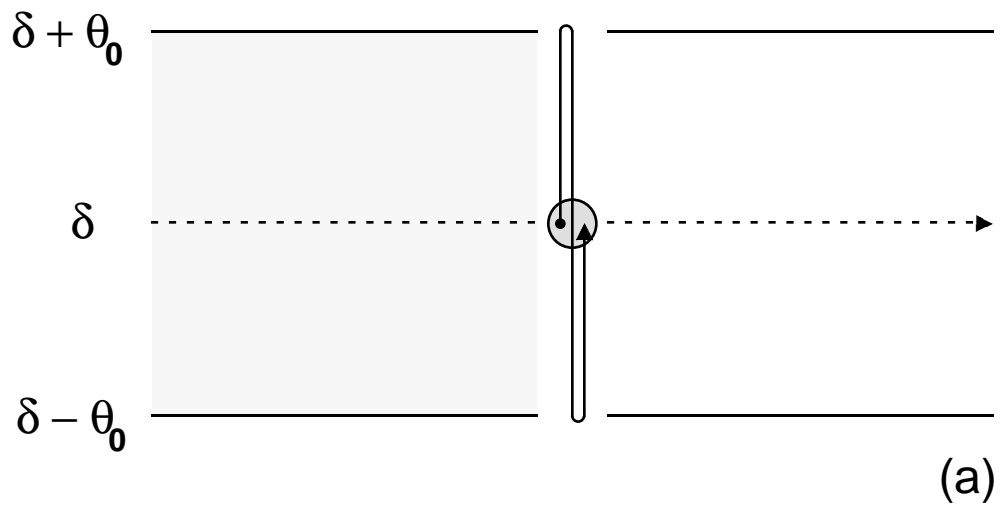


Fig. 1

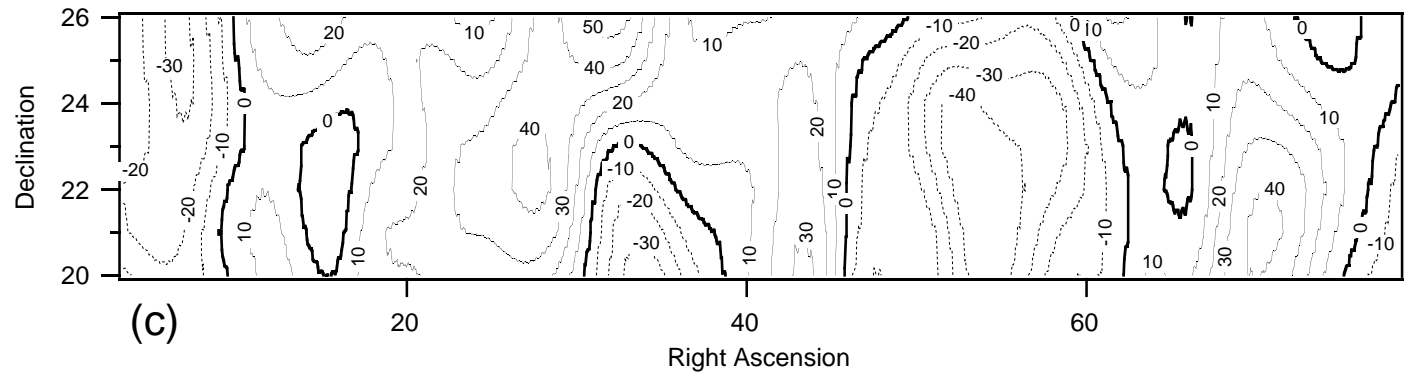
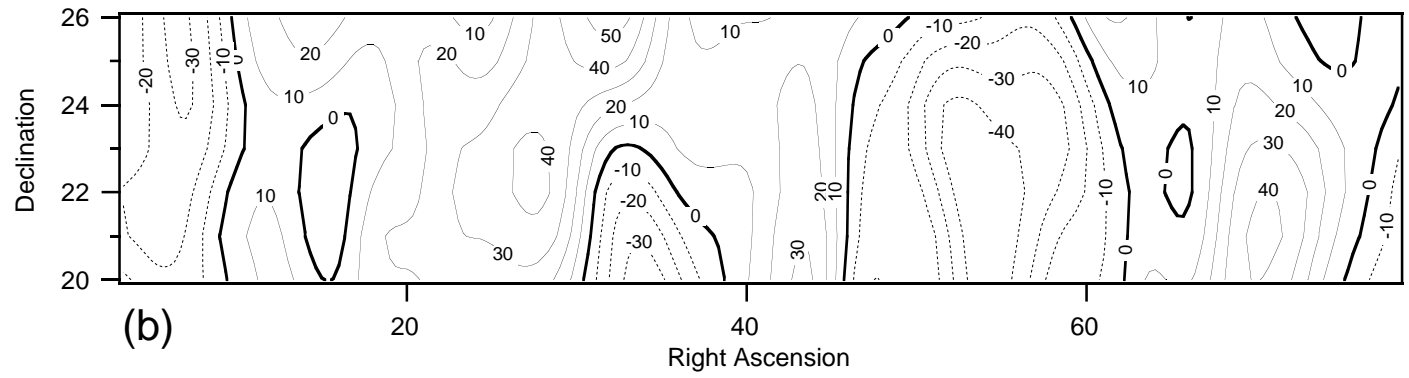
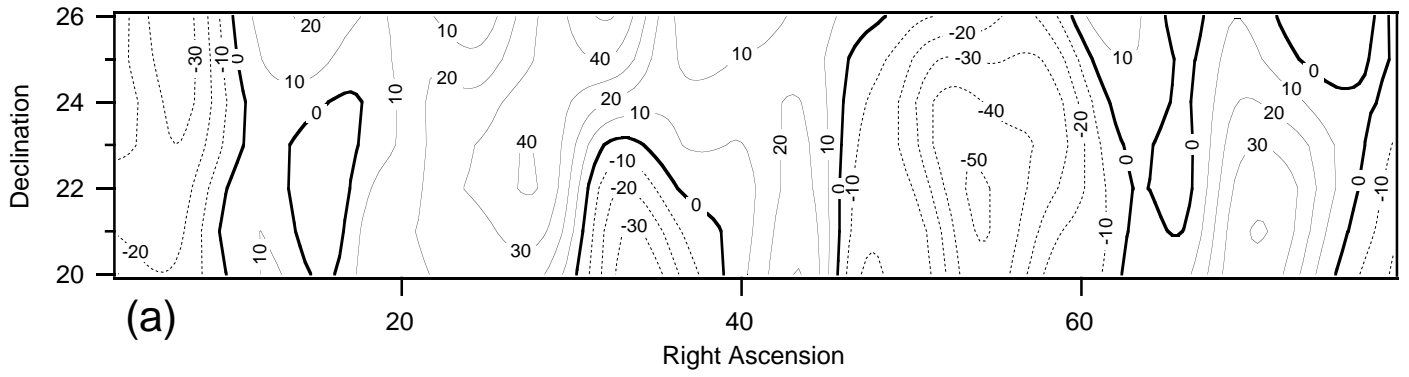


Fig. 2

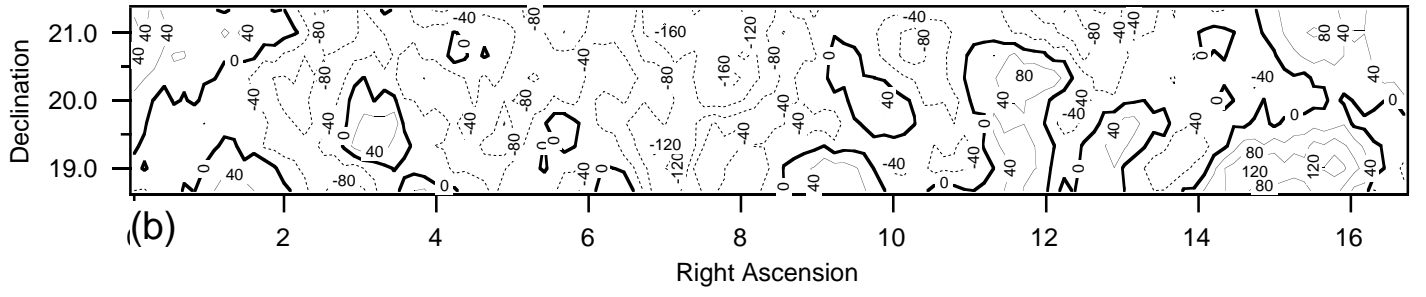
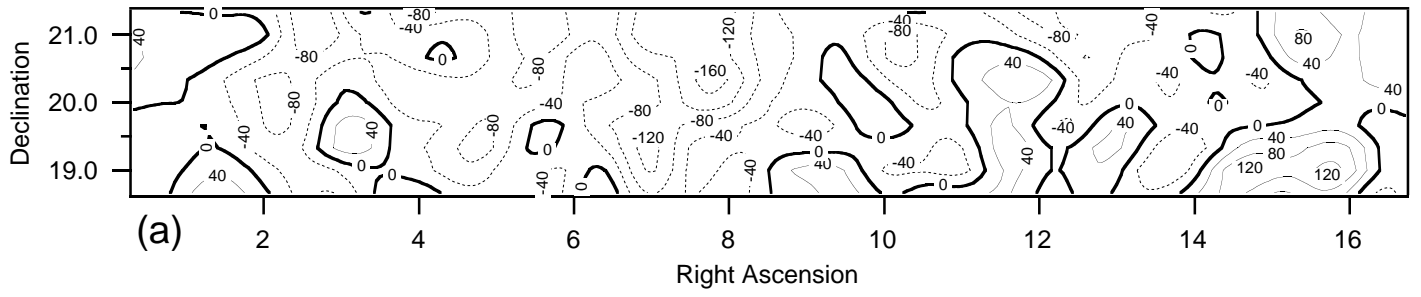


Fig. 3

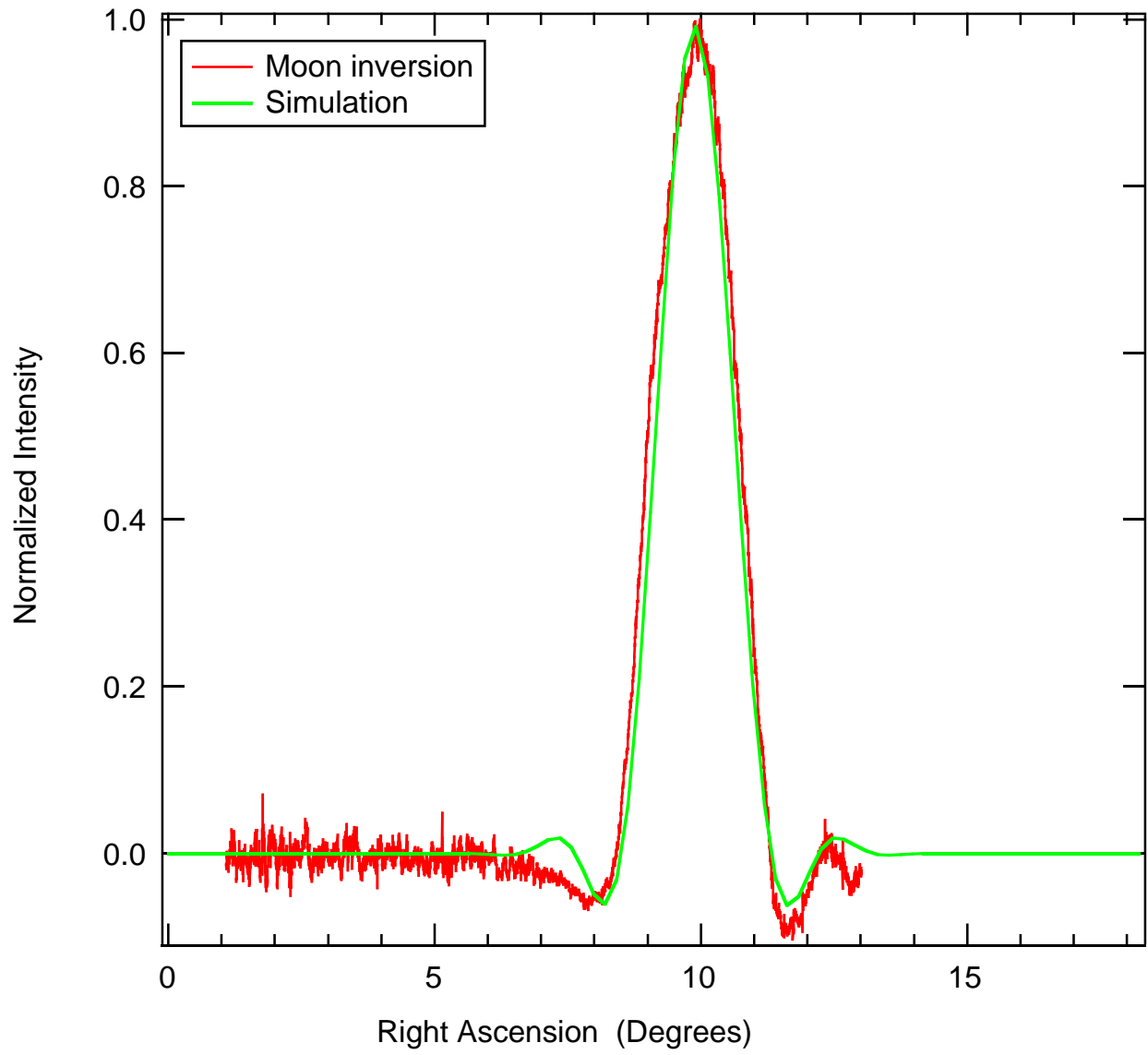


Fig 4